Surface composition of clean, epitaxial thin films of $YBa_2Cu_3O_{7-x}$ from quantitative x-ray photoemission spectroscopy analysis

G. Frank, Ch. Ziegler, and W. Göpel
Institute of Physical and Theoretical Chemistry, University of Tübingen, D-7400 Tübingen, Federal Republic of Germany
(Received 20 July 1990)

Angle-dependent x-ray photoemission spectra (XPS) of epitaxial thin-film $YBa_2Cu_3O_{7-x}$ show characteristic reversible and distinct changes with different surface treatments. These changes are analyzed by applying a new model for the quantitative XPS analysis, which takes into consideration the anisotropic structure of *c*-axis-oriented $YBa_2Cu_3O_{7-x}$. The analysis makes it possible to differentiate between different elemental compositions of the outer layers in the surface unit cell. Evaluations of our experimental data indicate that only surfaces with a nominal BaO and CuO layer composition exist in the outermost atomic layer.

INTRODUCTION

During the last three years, since the discovery of the high-T_c superconductor $YBa_2Cu_3O_{7-x}$, there have been great efforts in trying to understand the electronic bulk properties of this material based upon results from photoelectron spectroscopy.[1–11] For this purpose, "ideal" surfaces have to be prepared which should show bulk characteristics over the photoemission analysis depth. To prepare such surfaces from pellet and single-crystal materials, mechanical cleaning such as cleaving or scraping is commonly used. Surfaces of thin films have often been studied as-prepared and only one group tried a chemical etching cleaning procedure.[12,13]

Because of inherent problems in the surface cleaning procedure, only a few photoemission measurements are available on clean, well-defined surfaces of cleaved single crystals or oriented thin films.[9–11,14,15] The exact line shapes and binding energies for the x-ray photoemission spectroscopy (XPS) photoelectron lines in particular are not yet established. The published values of binding energies, e.g., for the Ba $3d_{5/2}$ bulk peak, differ at least to within 0.6 eV. Also the origin of the high-binding-energy components of the barium and oxygen XPS core peaks is not quite clear. Some authors assign these components to contaminations at the grain boundaries or the surface,[3,16–18] others to a nonsuperconducting surface phase[12,13,19–22] formed in the absence of any contamination.

In the first part of this paper we report on systematic work to optimize a nondestructive *in situ* cleaning method for thin films. It is based upon heating in ultrahigh vacuum (UHV), treatment in pure oxygen, and an XPS analysis of the elemental composition.

In the second part we present a refined model for the quantitative determination of elemental distributions in the first atomic layers of $YBa_2Cu_3O_{7-x}$, which is based upon results from angle-dependent XPS measurements. This will make it possible to determine the surface elemental compositions of differently prepared epitaxial $YBa_2Cu_3O_{7-x}$. The refined model takes into account that this material has a unit-cell dimension along the *c* axis which is between 0.8 and 2 times larger than the inelastic mean free path of photoelectrons utilized in the XPS analysis.

EXPERIMENTAL

The XPS studies were performed in a combined high-pressure-ultrahigh-vacuum system (for details see, e.g., Ref. 23) with a vacuum scientific workshop Ha 150 analyzer equipped with a Mg K_α source. The pass energy was set to 25 or 50 eV in different experiments with an overall resolution [full width at half maximum (FWHM) of Ag $3d_{5/2}$] of 1.0 and 1.45 eV, respectively. All spectra after each sample pretreatment cycle were taken at room temperature.

The base pressure during analysis was below 3×10^{-8} Pa. This was also the base pressure in a separate preparation chamber for the high-pressure oxygen exposure experiment.

The investigated samples were epitaxial films of $YBa_2Cu_3O_{7-x}$ with a thickness of 200 nm on $SrTiO_3$ (100) or MgO (100) with $T_{c,0} > 87$ K and J_c (77 K) $> 10^6$ A/cm^2. The bulk geometric structure was checked by x-ray diffraction and Rutherford backscattering spectroscopy (RBS).[24,25] The *c* axis of $YBa_2Cu_3O_{7-x}$ was oriented perpendicular to the surface.

Immediately after inserting the samples into the UHV chamber, XPS spectra were taken from each sample. Then the samples were heated in UHV until the total amount of carbon was less than 1.5 at. % as checked by XPS. In some cases, only temperatures less than 520–570 K K were needed. For these samples no further annealing was necessary.[4,26] In other cases, temperatures up to 670–720 K had to be applied, which caused the orthorhombic-to-tetragonal phase transition. This transition can be observed in the Cu $2p_{3/2}$ XPS feature for which the satellite-to-main-peak ratio is reduced to below 0.4. To readjust the superconducting phase these samples were subsequently annealed in 99.9996% pure oxygen at temperatures between 690 and 750 K and pressures between 5×10^1 and 1×10^4 Pa. The gas had to be

purified carefully prior to this treatment by passing the oxygen over a liquid-nitrogen trap and thereby freezing out possible amounts of water or CO_2. The annealing temperature was checked by a Pt/Pt (10%Rh) thermocouple in direct contact with the sample surface. It was covered by a thin platinum foil to avoid catalytically induced reactions of $YBa_2Cu_3O_{7-x}$ with rhodium.

The XPS binding energies are referred to the Fermi level of platinum. The energy scale was calibrated in a linear regression with 17 reference levels covering the energy range up to 1000 eV. This calibration leads to an absolute accuracy better than 0.1 eV in the energy region of core-level emissions to be discussed now.[27]

For the quantitative analysis, an S-shaped background was subtracted,[28] the $K_{\alpha 3,4}$ satellite peaks were subtracted, and all many-body-effect satellites were taken into account. The analyzer function was determined experimentally.[27] The geometry of the sample arrangement and the acceptance angle of the spectrometer were also taken into account.[29,30]

The decomposition of the barium and oxygen lines was performed using Gaussian-shaped peaks. The linewidths of barium differ less than 8% for the surface and bulk component, respectively. This difference in the linewidth was established from independent measurements of samples which were dominated by only one component. This difference in the linewidth was observed in more than 50 independent measurements. Consistent results were obtained for both the Ba $3d_{5/2}$ and Ba $4d_{5/2}$ emissions. The use of additional Lorentzian components in the peak shape analysis decreases the least-squares deviations between experimental and calculated values by a factor of 0.9 without changing the values of binding energies and intensities within the experimental error bars.

MODEL FOR XPS QUANTITATIVE ANALYSIS OF $YBa_2Cu_3O_{7-x}$

For a homogeneous substrate covered by a thin homogeneous layer, the overlayer model can be applied:[29,30]

$$\frac{I_{\mathrm{OL}}}{I_s}=\frac{N_{\mathrm{OL}}\lambda_{\mathrm{OL}}(E_{\mathrm{kin,OL}})\sigma_{\mathrm{OL}}L_{\mathrm{OL}}(\beta)\{1-\exp[-d/\lambda_{\mathrm{OL}}(E_{\mathrm{kin,OL}})]\}}{N_s\lambda_s(E_{\mathrm{kin},s})\sigma_s L_s(\beta)\exp[-d/\lambda_{\mathrm{OL}}(E_{\mathrm{kin},s})]}\ . \tag{1}$$

Here, I is the measured intensity, N the number of atoms in the overlayer (OL) and the substrate (s), $\lambda(E_{\mathrm{kin}})$ the inelastic mean free path (IMFP) for electrons with kinetic energy E_{kin} in the material which can be calculated using specific material parameters such as mass density, number of electrons in the valence band, and atomic mass[31,32] within 20–30 % accuracy, σ the cross section, and $L(\beta)$ the angular asymmetry with β as symmetry parameter; the latter three are given in the literature.[33,34]

This model assumes knowledge about the surface layer elemental composition as a prerequisite to perform precise calculations of the layer thickness. It leads to reliable results about the thickness of the subsurface elemental composition, especially for systems where one kind of atoms appears in both, the overlayer and the substrate, with the two corresponding peaks well separated by a pronounced chemical shift. Then σ and L cancel and Eq. (1) can be simplified.

An important assumption in this model is that the different atoms are distributed uniformly over the probed depth of the sample. Considering the anisotropic structure of $YBa_2Cu_3O_{7-x}$ this assumption is not justified at all. As can be deduced from Fig. 1, the yttrium atoms are separated by 1.17 nm along the c axis and even the other elements are not uniformly distributed, i.e., the distance between two layers which contain the same type of atoms is not negligible compared to the inelastic mean free path (IMFP) of the photoelectrons, with energy-dependent values between 0.8 and 2 nm. Nevertheless this model had already been applied to characterize the elemental composition of as-prepared, contaminated $YBa_2Cu_3O_{7-x}$ thin films[17,19,20] and cleaved single crystals.[14]

In the following refinement of the above-mentioned standard model of quantitative XPS analysis we assume a perfectly c-axis-oriented structure for $YBa_2Cu_3O_{7-x}$. There are six different possibilities of forming a surface with a uniform lateral elemental constitution, which are summarized in Table I. Taking into account the distances between the different layers from data on the bulk crystal structure of $YBa_2Cu_3O_{7-x}$,[35,36] the intensities of core-level emissions can be calculated from

$$I_x=J_0A_0T(E_{\mathrm{kin}})D(E_{\mathrm{kin}})\sigma_x\sum_{i=1}^{\infty}\int_{\Delta\Omega}d\Omega\cos\alpha\int_{-\Delta z}^{\Delta z}dz'M(\alpha;\psi,\beta)N_x(z')\exp[-(z_i+z')/\lambda(E_{\mathrm{kin}})\cos\alpha] \tag{2}$$

with the modified cross section as defined by[37]

$$M(\alpha;\psi,\beta)=\frac{1}{4\pi}\left[1-\frac{\beta}{8}(3\cos^2\psi-1)(3\cos^2\alpha-1)\right] \tag{3}$$

and I_x as the intensity of the core level of element x, J_0 the photon flux, A_0 the detected area, $T(E_{\mathrm{kin}})$ the analyzer function, $D(E_{\mathrm{kin}})$ the detector function, $\Delta\Omega$ the acceptance angle of the analyzer, α the angle between surface normal and analyzer axis, σ the cross section for subshell ionization,[33] ψ the angle between photon source and analyzer, β the asymmetry parameter,[34] $N_x(z')$ the distribution of the element x along the c axis, and λ the inelastic mean free path.[31,32]

The sum in Eq. (2) is taken over all distances between the layers of one element from the surface to the total in-

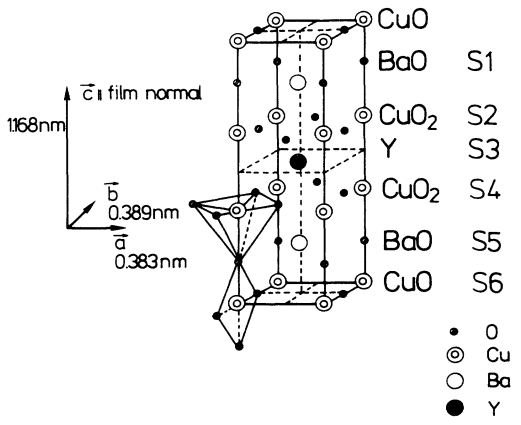

FIG. 1. Geometric structure of $YBa_2Cu_3O_{7-x}$. The chemical compositions CuO, BaO, etc. characterize elements in six different layers $S1$–$S6$ parallel to the surface of our films according to Table I.

formation depth [assumed as 7λ according to the American Society for Testing and Materials (ASTM) Committee E42 (Ref. 38)]. The integration over z' extends over $2z=0.04$ nm, i.e., the assumed spatial extent of the investigated inner core-level orbitals Cu $2p$, Ba $3d$, O $1s$, and Ba $4d$ along the c axis. For simplification the spatial distribution of the electrons within the orbitals was assumed to be constant, i.e., the variation of the radial wave function with distance from the nucleus is neglected. Detailed calculations show that the assumed extension of the core levels has only a small influence on the total intensity results and the difference between calculations using extended core-level orbitals and pointlike orbitals is less than 2%. The spatial extension of the orbitals may, however, become important in other situations, where valence or core levels with low binding energies are investigated.

As the absolute value of the photon flux J_0 is not known, only relative intensities will be calculated in the following. Theoretical results for photoelectron intensities normalized to the most intense XPS peak (Ba $3d_{5/2}$) are listed in the lower part of Table I for the different possible near-surface layer compositions as listed in the upper part of this table. Taking these results for the photoelectron intensities of the core levels to calculate this stoichiometry in the usual way [similar to Eq. (1)], results are obtained which are significantly different from the ideal ratio 1:2:3 for the c-axis-oriented $YBa_2Cu_3O_{7-x}$.

The overall uncertainty of the calculations is better than 15%. This takes into account the known uncertainties of the tabulated values of σ, β, and λ.[31–34] In addition it takes into account that the values used for estimating the angular asymmetry and the cross section are tabulated only for randomly oriented atoms, whereas our model assumes atoms in a fixed orientation. The systematic differences resulting from this inaccuracy affect the different core-level intensities within one layer sequence, but the differences for one specific core level between the six different layer sequences remain unaffected. Neglecting the influence of elastic scattering leads to uncertainties between 15 and 30% in the absolute photoelectron intensities depending on the sample morphology as shown in the literature, but for relative photoelectron intensities as used in our calculations the influence is certainly smaller than 15%.[31]

Even by accepting the value of 15% for the maximum uncertainty of our theoretical calculations of relative photoelectron intensities for $YBa_2Cu_3O_{7-x}$ core levels, the differences in the intensity of one specific core level are nevertheless significant for the six layer sequences summarized in Table I (for instance, 130% for Cu $2p_{3/2}$ and even 25% for Ba $4d$). The model predicts pronounced differences in the different theoretical near-surface layer compositions well above theoretical or experimental uncertainties. In the following discussion we will therefore apply this model to determine the surface

TABLE I. Different theoretical models ($S1$–$S6$) to form a surface of a perfect c-axis-oriented $YBa_2Cu_3O_7$ sample and calculated relative photoemission intensities for the denoted lines according to Eq. (2).

Models layer composition	$S1$	$S2$	$S3$	$S4$	$S5$	$S6$	Random
	BaO	CuO_2	Y	CuO_2	BaO	CuO	
	CuO_2	Y	CuO_2	BaO	CuO	BaO	
	Y	CuO_2	BaO	CuO	BaO	CuO_2	
	CuO_2	BaO	CuO	BaO	CuO_2	Y	
	BaO	CuO	BaO	CuO_2	Y	CuO_2	
	CuO	BaO	CuO_2	Y	CuO_2	BaO	
	BaO	CuO_2	Y	CuO_2	BaO	CuO	
Peak	Calculated relative XPS intensities						
Cu $2p_{3/2}$	0.74	1.47	0.96	1.01	0.63	1.14	0.94
Ba $3d_{5/2}$	1.00	1.00	1.00	1.00	1.00	1.00	1.00
O $1s$	0.31	0.49	0.37	0.35	0.26	0.37	0.36
Y $3d$	0.11	0.19	0.17	0.09	0.08	0.12	0.11
Ba $4d$	0.19	0.24	0.22	0.21	0.18	0.21	0.21

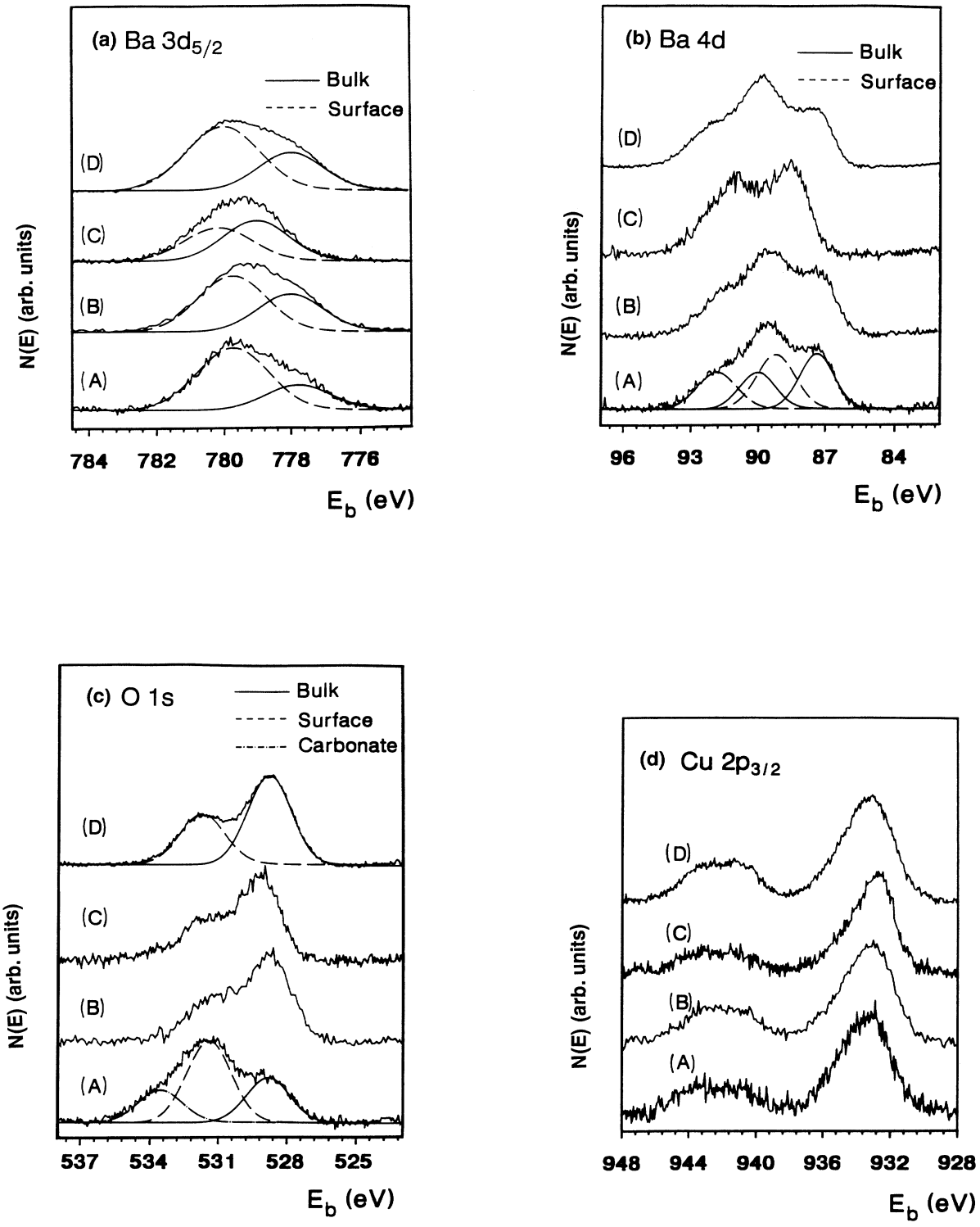

FIG. 2. XPS spectra (after subtraction of an S-shaped background and $K_{\alpha 3,4}$ satellite contribution) and peak fit analysis of (a) Ba $3d_{5/2}$, (b) Ba $4d$, (c) O $1s$, and (d) Cu $2p_{3/2}$. Spectra are shown of unpretreated samples (A), after heating the samples in UHV to 520 K (B), after heating in UHV to 650 K (C), and after annealing in 5×10^3 Pa pure oxygen at 700 K (D). All spectra were taken at room temperature in UHV.

elemental compositions of our samples with various different pretreatment procedures.

RESULTS AND DISCUSSION

Photoemission of electrons was monitored of the core levels Cu $2p_{3/2}$, Ba $3d_{5/2}$, O 1*s*, Y $3p_{3/2}$, C 1*s*, Y 3*d* and Ba 4*d* at 0° and 70° relative to the surface normal. Changes in the line shapes after different treatments are summarized in Fig. 2. Spectra denoted by "A" correspond to samples which are freshly inserted into the UHV chamber. From the O 1*s* line shape we deduce the samples to be covered by contaminations such as OH groups, carbonoxides, and carbonates.[17,21,22] However, in most samples there is no contribution to the Ba $3d_{5/2}$ peak at energies around 782 eV, where the barium carbonate peak is expected.[20–22,39]

Gentle heating in UHV up to 520 K leads to spectra denoted by "B." After this treatment small amounts of carbon less than 3 at. % remain. The O 1*s* peak shows the typical form for $YBa_2Cu_3O_{7-x}$,[1,3,5,6,12–14] with the main feature at 528.6 eV. The weak part at 531.5 eV is associated with a surface component as can be derived from comparative measurements at 0° and 70°. A surface component is also a common feature in the barium peaks with the low-binding-energy part associated with the superconductor's bulk structure[1,3,9,12–14,17,18,22] and the high-binding-energy part associated with the surface structure. The two peaks are separated by 1.8 eV. The core-level spectrum of Cu $2p_{3/2}$ shows a satellite structure at around 942 eV which is typical for divalent copper.[1,4,9,14,15]

Further heating in UHV up to 650 K leads to spectra denoted by "C" with their decreased surface components in the barium and oxygen peak range. In addition we observe a decrease of the Cu $2p_{3/2}$ satellite which can be attributed to a loss of oxygen. The influence of the oxygen loss on the binding energies of the barium bulk components is discussed in detail elsewhere.[26]

The last set of spectra denoted by "D" shows the influence of an *in situ* annealing in ultrapure oxygen. No further contamination with carbon can be seen to within the sensitivity of our XPS analysis. The measurements at large angles show an oxygen-to-carbon ratio larger than 100, corresponding to less than $\frac{1}{5}$ a monolayer of carbon.[7,8] The high-binding-energy components of barium and oxygen increase as compared with results from spectra "C." The line shapes of the barium peaks are comparable to those from spectra A and B.

The intensity ratios referred to Ba $3d_{5/2}$ of spectra B, C and D can be compared directly with results from our calculations because the attenuation of the $YBa_2Cu_3O_{7-x}$ peaks due to carbon contamination is negligible. The measured relative intensities of the photoelectron lines show significant deviations after the different treatments leading to spectra A–D, although the volume stoichiometry 1:2:3 of the metal atoms is not expected to change during the sample pretreatments applied in our work. The latter follows from the thermodynamic estimations.

In order to clarify the origin of these differences, the measured intensity ratios of the observed core levels are compared with those calculated for the different hypothetic surface structures of Table I on the basis of the model discussed in the previous chapter. The analysis is performed by taking the sum of the squared deviations between the measured and the calculated intensity ratios, χ^2. The surface composition model leading to the smallest value of χ^2 is assumed to describe the real sample surface composition. The χ^2 values, normalized to the best value, are shown in Table II for the different experimental surface treatments with the absolute value of the best χ^2 better than 0.1. This indicates a high confidence level of the data evaluation procedure.

Measurements of various samples and several repeated cycles using the same pretreatment on one sample always lead to the same relative XPS intensities. From this we conclude to have applied experimental conditions to adjust reproducibly the elemental composition in the outermost surface layers.

The surface morphology was characterized by scanning electron microscopy. The surface contains large, smooth areas covered by small droplets. The droplets cover between 8 and 20 % of the surface. To check possible systematic errors in the evaluation of XPS results due to the influence of deviating chemical composition in the droplets, spatial resolved scanning Auger electron spectroscopy (AES) measurements were performed and compared to nonspatial resolved results from integrated AES measurements for a "droplet-rich" sample. The latter data represent an average composition. To estimate the influence of the droplets on our XPS results the AES intensities of Ba *MNN*, Cu *LMM*, and Y *LMM* were normalized to the Ba *MNN* intensities and then compared for both the spatial resolved and the averaged measurements with intensity ratios Ba:Cu:Y=1:1.36:0.15 for the averaged measurements, and 1:1.27:0.16 for the flat parts resulting from $YBa_2Cu_3O_{7-x}$ and 1:1.56:0.15 resulting

TABLE II. Comparison of experimental relative photoemission intensities with the calculated intensities of Table I by means of the least-squares deviations χ^2/χ^2_{best}. The notation of the samples is taken from Fig. 1.

	Models						
Treatment	*S*1	*S*2	*S*3	*S*4	*S*5	*S*6	Random
B	27.4	77.3	5.7	1.0	46.3	6.7	3.3
C	1.0	134.1	12.2	17.5	5.3	39.7	17.0
D	3.7	114.2	21.4	25.7	1.0	44.3	25.4

from the droplets. The difference in the yttrium content is negligible for the droplets and the flat areas. The difference in the content of copper and barium shows that the droplets are enriched with copper. We conclude that the difference between integrated relative intensity ratios and those of pure flat areas is below 8%. As the information depths of XPS and AES are comparable, the systematic error in the XPS measurements due to the influence from droplets is also below 8%. This value is in the range of the experimental error to calculate the correct core-level intensities. We therefore conclude that the observed changes in the measured intensities after different sample treatments given in Fig. 2 and Table II are not significantly influenced by the droplets and the experimental XPS data can be analyzed according the model developed in the chapter before.

Comparing all the results in Tables I and II we deduce the existence of one or two layers "$BaCuO_2$" at the surface which may either result from a specific surface atom composition of ideal $YBa_2Cu_3O_{7-x}$ or from the existence of a separate surface phase of the composition "$BaCuO_2$". In line with the latter interpretation are results on experimental binding energies of the barium $3d_{5/2}$ and $4d_{5/2}$ core levels. As mentioned above, the corresponding XPS peaks show contributions from a bulk and an additional surface component whenever $YBa_2Cu_3O_{7-x}$ surfaces are prepared by heat treatment in the presence of oxygen. The binding energies of the surface component agree well with data from a $BaCuO_2$ standard,[21] but it is not yet clear whether such thin layers as observed in our experiments show ideal bulk characteristics of this material.[26]

In contradiction to this assumption are the crystallographic data on $BaCuO_{2+x}$.[40,41] It crystallizes with a very large cubic cell of dimension 1.827 nm. The unit cell is formed by 360 atoms and shows a very complicated structure which does not fit with the crystal parameters of $YBa_2Cu_3O_{7-x}$. The dimensions of the $BaCuO_2$ unit cell is pronounced larger than the nominal thickness of the "$BaCuO_2$" surface layer observed in our experiments. The thickness of the surface component of $YBa_2Cu_3O_{7-x}$ was estimated from data on the layer distances in bulk $YBa_2Cu_3O_{7-x}$ by assuming an equal number of barium and copper oxide layers above the first yttrium layer. Results for the surface pretreatments of spectra "B" to "D" are given in Table III.

For comparison the values for the nominal thicknesses calculated from Eq. (1) are listed in Table III. These values are in the same range as other published values.[20] Comparing these values with those of our refined analysis shows that the simplifications in Eq. (1) lead to a slight overestimation of the layer thickness. Nevertheless all of these thickness values of the overlayer are smaller than the length of one unit cell of bulk $BaCuO_2$.

We therefore conclude that no separate homogeneous $BaCuO_2$ phase exists at the $YBa_2Cu_3O_{7-x}$ surface of clean, epitaxial thin films. We assume thermodynamically preferred surface atom compositions to exist which depend on the oxygen partial pressure and the temperature.

TABLE III. Calculations of the surface layer ($BaCuO_2$) thickness according to Eq. (1) and according to the sum of layer distances for the best surface model of Table I, as calculated using crystal data of bulk $YBa_2Cu_3O_{7-x}$ (Ref. 36) and assuming an equal number of copper and barium layers on top of the first yttrium layer.

	Calculation method distances		
Treatment	Ba $3d_{5/2}$ Thickness (nm)	Ba $4d_{5/2}$	Sum of layer
A	1.37	1.00	
B	0.84	0.83	0.79
C	0.44	0.44	0.39
D	0.93	1.08	0.79

The surface compositions of the first unit cell according to structure *S*5 in Table I seem to be the most stable under the conditions chosen for all oxygen-exposed surfaces of films with their *c* axis perpendicular to the substrate surface unit cells. After gentle heating in UHV, structure *S*4 was observed. After strong heating in UHV the structure *S*1 is more preferred.

The bonds in the first surface unit cell are assumed to be different if compared with those in the bulk material. This leads to the observed XPS binding-energy shifts in the barium and oxygen peaks.

CONCLUSIONS

Our quantitative analysis of XPS data on smooth epitaxial thin films of $YBa_2Cu_3O_{7-x}$ makes it possible to distinguish different layer compositions in the surface unit cell and to detect surface phases. The model can easily be extended to other crystal orientations or other anisotropic materials.

On all $YBa_2Cu_3O_{7-x}$ samples examined in this study only surface unit cells with nominal BaO or CuO_2 top layers were observed.

The results reported here are important for the application of surface-sensitive techniques in the determination of geometric or electronic structures of bulk $YBa_2Cu_3O_{7-x}$. The observed different binding energies of surface and bulk components lead to the suggestion that also the electronic band structure is strongly influenced by the surface atom composition. This is in line with recent theoretical calculations.[42]

ACKNOWLEDGMENTS

The authors gratefully acknowledge P. Berberich, F. Baudenbacher, and H. Kinder, Technische Universität Munich, for sample preparation and measurements of the superconducting properties, W. Neu for excellent technical assistance during the performance of the experiments, and A. Hierlemann for help during the measurements. This work was partially supported by the Bundeminister für Forschung und Technologie, No. 13N5482, and the Land Baden Württemberg, Forschungsschwerpunkt "Oxidische Hoch-T_c Supraleiter."

[1]P. Steiner, V. Kinsinger, I. Sander, B. Siegwart, S. Hüfner, and C. Politis, Z. Phys. B **67**, 19 (1987).
[2]T. J. Wagener, Y. Gao, I. M. Vitomirov, C. M. Aldo, J. J. Joyce, C. Capasso, J. H. Weaver, and D. W. Capone II, Phys. Rev. B **38**, 232 (1988).
[3]H. M. Meyer III, D. M. Hill, T. J. Wagener, Y. Gao, J. H. Weaver, D. W. Capone II, and K. C. Goretta, Phys. Rev. B **38**, 6500 (1988).
[4]S. L. Qiu, M. W. Ruckman, P. D. Johnson, J. Chen, L. Jiang, C. L. Lin, M. Strongin, B. Sinovic, and N. Brookes, in *Thin Film Processing and Characterization of High-Temperature Superconductors,* Proceedings of the American Vacuum Society Topical Conference on Thin Film Processing and Characterization of High-T_c Superconductors, AIP Conf. Proc. No. 165, edited by G. Lucovsky (AIP, New York, 1988), pp. 245-253.
[5]H. M. Meyer III, D. M. Hill, J. H. Weaver, D. L. Nelson, and K. C. Goretta, Appl. Phys. Lett. **53**, 1004 (1988).
[6]H. M. Meyer III, Y. Gao, T. J. Wagener, D. M. Hill, J. H. Weaver, B. K. Flandermeyer, and D. W. Capone II, *Thin Film Processing and Characterization of High-Temperature Superconductors* (Ref. 4), pp. 254–263.
[7]W. R. Flawell and R. G. Egdell, Phys. Rev. B **39**, 231 (1989).
[8]R. G. Egdell and W. R. Flawell, Z. Phys. B **74**, 279 (1989).
[9]H. M. Meyer III, D. M. Hill, T. J. Wagener, J. H. Weaver, C. F. Gallo, and K. C. Goretta, J. Appl. Phys. **65**, 3130 (1989).
[10]R. Liu, C. G. Olson, A. -B. Yang, C. Gu, D. W. Lynch, A. J. Arko, R. S. List, R. J. Bartlett, B. W. Veal, J. Z. Liu, A. P. Paulikas, and K. Vandervoort, Phys. Rev. B **40**, 2650 (1989).
[11]Y. Sakisaka, T. Komeda, T. Maruyama, M. Onchi, H. Kato, Y. Aiura, H. Yanashima, T. Terashima, Y. Bando, I. Iijima, K. Yamamoto, and K. Hirata, Phys. Rev. B **39**, 2304 (1989).
[12]R. P. Vasquez, B. D. Hunt, and M. C. Foote, Appl. Phys. Lett. **53**, 2692 (1988).
[13]R. P. Vasquez, M. C. Foote, and B. D. Hunt, Appl. Phys. Lett. **54**, 1060 (1989).
[14]D. E. Fowler, C. R. Brundle, J. Lerczak, and F. Holtzberg, J. Electron Spectrosc. Relat. Phenom. **52**, 323 (1990); Physica C **162-164**, 1303 (1989).
[15]D. van der Marel, J. van der Elp, G. A. Sawatzky, and D. Heitmann, Phys. Rev. B **37**, 5136 (1988).
[16]W. K. Ford, J. Anderson, G. V. Rubenacker, J. E. Drumheller, C. T. Chen, M. Hong, J. Kwo, and S. H. Liou, J. Mater. Res. **4**, 16 (1988).
[17]J. Halbritter, P. Walk, H. -J. Mathes, B. Haeuser, and H. Rogalla, Z. Phys. B **73**, 277 (1988).
[18]D. C. Miller, D. E. Fowler, C. R. Brundle, and W. Y. Lee, in *Thin Film Processing and Characterization of High-Temperature Superconductors* (Ref. 4), pp. 336–348.
[19]X. D. Wu, A. Inam, M. S. Hedge, T. Venkatesan, C. C. Chang, E. W. Chase, B. Wilkens and J. M. Tarascon, Phys. Rev. B **38**, 9307 (1988).
[20]C. C. Chang, M. S. Hedge, X. D. Wu, B. Dutta, A. Inam, T. Venkatesan, B. J. Wilkens, and J. B. Wachtman, Jr., Appl. Phys. Lett. **55**, 1680 (1989).
[21]F. Stucki, P. Brüesch, and T. Baumann, Physica C **153-155**, 200 (1988).
[22]S. Myrha, P. R. Chalker, P. T. Moseley, and J. C. Riviere, Physica C **165**, 270 (1990).
[23]W. Göpel, Sens. Act. **16**, 167 (1989).
[24]P. Berberich, J. Tate, W. Dietsche, and H. Kinder, Appl. Phys. Lett. **53**, 925 (1988).
[25]F. Baudenbacher, H. Karl, P. Berberich, and H. Kinder, Verh. Dtsch. Phys. Ges. **25**, 1212 (1990).
[26]Ch. Ziegler, G. Frank, and W. Göpel, Z. Phys. B **81**, 349 (1990).
[27]C. J. Powell, N. E. Erickson, and T. E. Madey, J. Electron Spectrosc. Relat. Phenom. **17**, 361 (1979).
[28]D. A. Shirley, Phys. Rev. B **5**, 4709 (1972).
[29]A. Jablonski, Surf. Interface Anal. **14**, 659 (1989).
[30]C. S. Fadley, R. J. Baird, W. Siekhaus, T. Novakov, and S. A. L. Bergstroem, J. Electron Spectrosc. Relat. Phenom. **4**, 93 (1974).
[31]S. Tanuma, C. J. Powell, and D. R. Penn, Surf. Interface Anal. **11**, 577 (1988).
[32]S. Tanuma, C. J. Powell, and D. R. Penn, Surf. Sci. **192**, L849 (1987).
[33]J. H. Scofield, J. Electron Spectrosc. Relat. Phenom. **8**, 129 (1976).
[34]R. F. Reilman, A. Msezane, and S. T. Manson, J. Electron Spectrosc. Relat. Phenom. **8**, 389 (1976).
[35]G. Roth and G. Heger, KfK-Nachr. **19**, 147 (1987).
[36]A. Santoro, S. Miraglia, F. Beech, S. A. Sunshine, D. W. Murphy, L. F. Schneemeyer, and J. V. Waszczak, Mater. Res. Bull. **22**, 1007 (1987).
[37]A. Jablonski, M. F. Ebel, and H. Ebel, J. Electron Spectrosc. Relat. Phenom. **42**, 235 (1987).
[38]C. J. Powell, J. Electron Spectrosc. Relat. Phenom. **47**, 197 (1988).
[39]T. Venkatesan, X. D. Wu, A. Inam, M. S. Hegde, E. W. Chase, C. C. Chang, P. England, D. M. Hwang, R. Krchnavek, J. B. Wachtman, W. L. McLean, R. Levi-Setti, J. Chabala, and Y. L. Wang, in *Chemistry of High-Temperature Superconductors II,* ACS Symposium Series, edited by D. L. Nelson and Th. F. George (American Chemical Society, Washington, D.C., 1988) Vol. 377, pp. 234–264.
[40]R. Kipka and H. Müller-Buschmann, Z. Naturforsch. Teil B **32**, 121 (1977).
[41]M. F. Weller and D. R. Lines, J. Chem. Soc. D **8**, 484 (1989).
[42]C. Calandra, G. Goldoni, F. Manghi, and R. Magri, Surf. Sci. **211/212**, 1127 (1989).